



This is an open access article distributed under the terms of the Creative Commons Attribution 4.0 International License (CC BY 4.0), which permits use, distribution, and reproduction in any medium, provided the original publication is properly cited. No use, distribution or reproduction is permitted which does not comply with these terms.

MODELLING OF DYNAMIC STATES OF FIVE-PHASE INDUCTION MOTOR

Pavel Záskalický*, Daniela Perduková, Jan Kaňuch

Faculty of Electrical Engineering and Informatics, Technical University of Kosice, Kosice, Slovakia

*E-mail of corresponding author: pavel.zaskalicky@tuke.sk

Pavel Záskalický 0000-0001-7335-8458,
Jan Kaňuch 0000-0001-5723-0198

Daniela Perduková 0000-0002-2856-2027,

Resume

In this paper is presented a mathematical model of a five-phase induction motor with a cage rotor and a stator coils connected to a star. In constructing the mathematical model, It is assumed that the motor is fed from a five-phase frequency converter with an ideal harmonic waveform of the output supply voltage. It is considered that the motor operates in an open control loop with the ability to control the frequency and amplitude of the supply voltage.

The basic voltage equations in a two-phase coordinate system coupled to a stator are derived, as well as the relation for the electromagnetic moment. Based on the parameters measured on a real motor, a dynamic model was implemented in Matlab-Simulink environment. Using the dynamic model, various motor operating states were simulated, such as frequency ramp-up, speed reversal, or operation at super-nominal frequencies.

Article info

Received 19 June 2025

Accepted 18 September 2025

Online 7 October 2025

Keywords:

induction motor
mathematical model
five-phase motor
MATLAB Simulink
dynamic states

Available online: <https://doi.org/10.26552/com.C.2025.053>

ISSN 1335-4205 (print version)
ISSN 2585-7878 (online version)

1 Introduction

With the evolution of power semiconductor converters, multiphase motors have gained increasing importance - most commonly five- or six-phase machines. Among them the five-phase motors offer significantly more advantages than their three- or six-phase counterparts.

A key benefit is the reduction of stator current for the same power output. This results in a decreased current load on the converter's semiconductor components as well as lower Joule losses in the stator windings. This advantage becomes particularly important in high-power motor applications [1].

The five-phase motors are also known for their quiet operation, making them suitable for installations in residential buildings, hospitals, and hotels where the low noise levels are critical. Another benefit is their fault-tolerant capability: they can continue operating even if one supply phase is lost. By appropriate phase-shifting the remaining supply voltages, a rotating magnetic field can still be produced. Although the motor operates with reduced power, functionality is preserved. In contrast,

a power loss in one phase of a three-phase motor typically leads to total failure. This makes the five-phase motors ideal for applications such as elevator drives in high-rise or medical buildings, where unexpected stoppages can cause serious disruption.

An additional important advantage is their higher efficiency compared to similarly rated three-phase motors [2-5].

Increasing the number of supply phases also increases electromagnetic torque for a motor of the same physical volume. This necessitates the development of appropriate mathematical methods to assess the performance benefits of five-phase machines [6-9].

Typically, the five-phase motors are powered by a five-phase voltage source inverter using pulse-width modulation (PWM) of the output voltage. When the modulation frequency is sufficiently high, the output voltage and current waveforms of the inverter can be considered harmonic in nature [3, 10-11].

The inverter circuit supplying five-phase motors consists of five legs, each made up of series-connected transistors with anti-parallel freewheeling diodes, as shown in Figure 1.

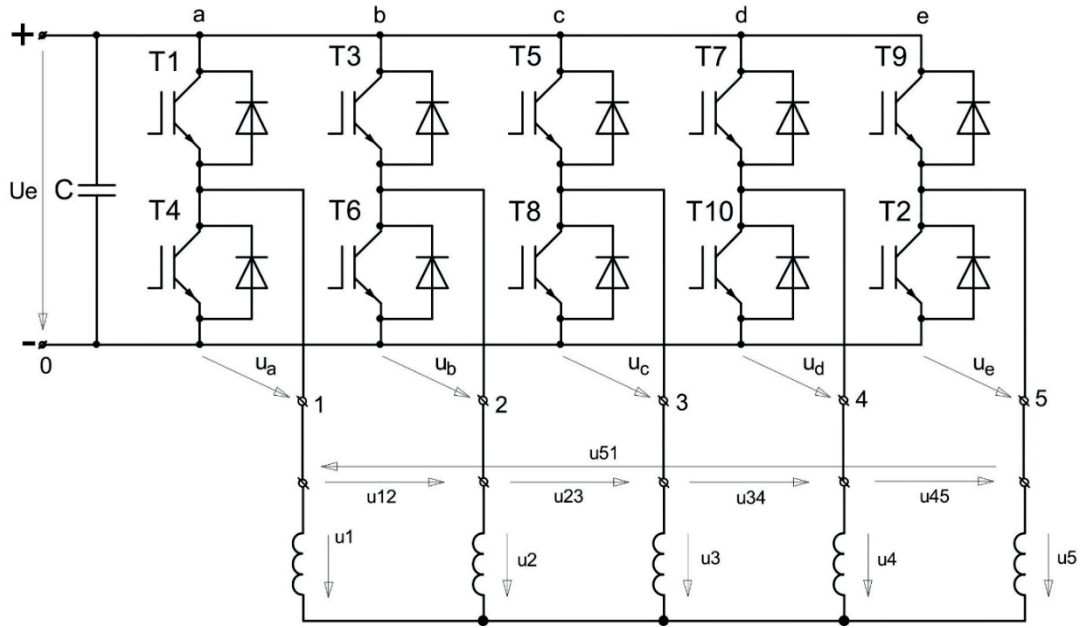


Figure 1 Five-phase voltage source inverter

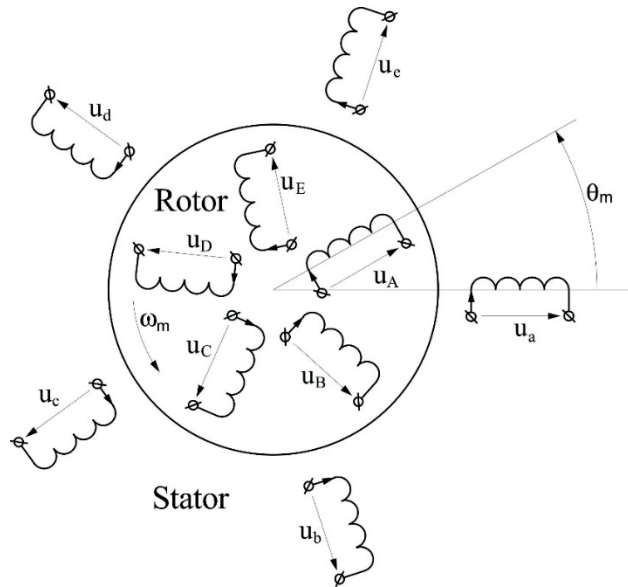


Figure 2 Windings of a five-phase machine

2 Mathematical model of a five-phase IM

When building the mathematical model of a motor, one starts from the two-pole version and assumes a motor with a wound armature, as shown in Figure 2. [12-14], where: $u_a, u_b, u_c, u_d,$ and u_e are the stator supply voltages. u_A, u_B, u_C, u_D and u_E are the rotor supply voltages.

The following voltage equations are valid for the motor stator coils:

$$\begin{aligned} u_a &= R_a i_a + \frac{d\psi_a}{dt}; u_b = R_b i_b + \frac{d\psi_b}{dt}; \\ u_c &= R_c i_c + \frac{d\psi_c}{dt}; u_d = R_d i_d + \frac{d\psi_d}{dt}; \\ u_e &= R_e i_e + \frac{d\psi_e}{dt}. \end{aligned} \quad (1)$$

Similarly, for the rotor windings:

$$\begin{aligned} u_A &= R_A i_A + \frac{d\psi_A}{dt}; u_B = R_B i_B + \frac{d\psi_B}{dt}; \\ u_C &= R_C i_C + \frac{d\psi_C}{dt}; u_D = R_D i_D + \frac{d\psi_D}{dt}; \\ u_E &= R_E i_E + \frac{d\psi_E}{dt}. \end{aligned} \quad (2)$$

where: R_{abcde} and R_{ABCDE} are the resistances of the stator and rotor coils, respectively;

i_{abcde} are the currents of the stator coils and i_{ABCDE} of the rotor coils, respectively;

ψ_{abcde} are the linkage fluxes of the stator coils and ψ_{ABCDE} of the rotor coils, respectively.

It is assumed that both the stator and rotor winding coils are symmetrical, so the coil resistances will be identical:

$$R_a = R_b = R_c = R_d = R_e = R_s; R_A = R_B = R_C = R_D = R_E = R_R.$$

The voltage Equations (1) and (2) can be expressed in the matrix form:

$$\begin{aligned} [u_{abcde}] &= R_s[i_{abcde}] + \frac{d}{dt}[\psi_{abcde}], \\ [u_{ABCDE}] &= R_R[i_{ABCDE}] + \frac{d}{dt}[\psi_{ABCDE}]. \end{aligned} \quad (3)$$

All the matrices in Equations (3) are column matrices.

For the linkage fluxes the following matrix equations are valid:

$$\begin{aligned} [\psi_{abcde}] &= [L_s][i_{abcde}] + [L_{SR}][i_{ABCDE}] \\ [\psi_{ABCDE}] &= [L_{SR}][i_{abcde}] + [L_R][i_{ABCDE}]. \end{aligned} \quad (4)$$

where, $[L_s]$ is stator, $[L_R]$ rotor and $[L_{SR}]$ stator-rotor matrix of inductances.

Matrix of stator inductances takes a form:

$$[L_s] = \begin{bmatrix} L_a & L_{ab} & L_{ab} & L_{ab} & L_{ab} \\ L_{ab} & L_a & L_{ab} & L_{ab} & L_{ab} \\ L_{ab} & L_{ab} & L_a & L_{ab} & L_{ab} \\ L_{ab} & L_{ab} & L_{ab} & L_a & L_{ab} \\ L_{ab} & L_{ab} & L_{ab} & L_{ab} & L_a \end{bmatrix} \quad (5)$$

where, L_a is a self-inductance and L_{ab} is a mutual inductance of stator windings.

Matrix of rotor inductances can be written as:

$$[L_R] = \begin{bmatrix} L_A & L_{AB} & L_{AB} & L_{AB} & L_{AB} \\ L_{AB} & L_A & L_{AB} & L_{AB} & L_{AB} \\ L_{AB} & L_{AB} & L_A & L_{AB} & L_{AB} \\ L_{AB} & L_{AB} & L_{AB} & L_A & L_{AB} \\ L_{AB} & L_{AB} & L_{AB} & L_{AB} & L_A \end{bmatrix} \quad (6)$$

where, L_A is a self-inductance and L_{AB} is a mutual inductance of rotor windings.

Matrix of stator-rotor mutual inductances depends on the rotor position:

$$[L_{SR}] = L_{aA} \begin{bmatrix} \cos \theta_m & \cos(\theta_m - \frac{2\pi}{5}) & \cos(\theta_m - \frac{4\pi}{5}) & \cos(\theta_m - \frac{4\pi}{5}) & \cos(\theta_m - \frac{2\pi}{5}) \\ \cos(\theta_m - \frac{2\pi}{5}) & \cos \theta_m & \cos(\theta_m - \frac{2\pi}{5}) & \cos(\theta_m - \frac{4\pi}{5}) & \cos(\theta_m - \frac{4\pi}{5}) \\ \cos(\theta_m - \frac{4\pi}{5}) & \cos(\theta_m - \frac{2\pi}{5}) & \cos \theta_m & \cos(\theta_m - \frac{2\pi}{5}) & \cos(\theta_m - \frac{4\pi}{5}) \\ \cos(\theta_m - \frac{4\pi}{5}) & \cos(\theta_m - \frac{4\pi}{5}) & \cos(\theta_m - \frac{2\pi}{5}) & \cos \theta_m & \cos(\theta_m - \frac{2\pi}{5}) \\ \cos(\theta_m - \frac{2\pi}{5}) & \cos(\theta_m - \frac{4\pi}{5}) & \cos(\theta_m - \frac{4\pi}{5}) & \cos(\theta_m - \frac{2\pi}{5}) & \cos \theta_m \end{bmatrix} = L_{aA}[C], \quad (7)$$

where $[C]$ is a matrix of cyclic rotor position and L_{aA} is a mutual inductance between the stator and rotor windings.

Finally, one can write the matrix equations for the stator and rotor linkage fluxes

$$\begin{aligned} [\psi_{abcde}] &= [L_s][i_{abcde}] + L_{aA}[C][i_{ABCDE}] \\ [\psi_{ABCDE}] &= L_{aA}[C]^t[i_{abcde}] + [L_R][\psi_{ABCDE}]. \end{aligned} \quad (8)$$

3 Voltages equations transformation

The transformation of the five-phase stator quantities into a two-phase system ($\alpha\beta xy0$) is realized using the transformation matrix $[A_s]$:

$$[A_s] = \begin{bmatrix} \cos(0) & \cos(\frac{2\pi}{5}) & \cos(\frac{4\pi}{5}) & \cos(\frac{6\pi}{5}) & \cos(\frac{8\pi}{5}) \\ \sin(0) & \sin(\frac{2\pi}{5}) & \sin(\frac{4\pi}{5}) & \sin(\frac{6\pi}{5}) & \sin(\frac{8\pi}{5}) \\ \cos(0) & \cos(\frac{6\pi}{5}) & \cos(\frac{12\pi}{5}) & \cos(\frac{18\pi}{5}) & \cos(\frac{24\pi}{5}) \\ \sin(0) & \sin(\frac{6\pi}{5}) & \sin(\frac{12\pi}{5}) & \sin(\frac{18\pi}{5}) & \sin(\frac{24\pi}{5}) \\ \frac{1}{2} & \frac{1}{2} & \frac{1}{2} & \frac{1}{2} & \frac{1}{2} \end{bmatrix}. \quad (9)$$

The transformation of the stator voltage Equations (3) is realized by multiplying them by the transformation matrix in Equation (9) from the left as follows:

$$[A_s][u_{abcde}] = R_s[A_s][i_{abcde}] + [A_s]\frac{d}{dt}[\psi_{abcde}], \quad (10)$$

where:

$$\begin{aligned} [A_s][u_{abcde}] &= [u_{\alpha\beta xy0}] \\ [A_s][i_{abcde}] &= [i_{\alpha\beta xy0}] \\ [A_s]\frac{d}{dt}[\psi_{abcde}] &= \frac{d}{dt}[\psi_{\alpha\beta xy0}]. \end{aligned}$$

For a symmetrical five-phase supply voltages system the following applies:

$$u_x = u_y = u_0 = 0.$$

Then, the stator voltages equations in the system ($\alpha\beta xy0$) take a form:

$$u_{\alpha s} = R_s i_{\alpha s} + \frac{d\psi_{\alpha s}}{dt}, u_{\beta s} = R_s i_{\beta s} + \frac{d\psi_{\beta s}}{dt}. \quad (11)$$

Transforming matrix for rotor quantities $[A_R]$ depends on the rotor position and takes a form:

$$[A_R] = \begin{bmatrix} \cos(\theta) & \cos\left(\theta_m - \frac{2\pi}{5}\right) & \cos\left(\theta_m - \frac{4\pi}{5}\right) & \cos\left(\theta_m - \frac{6\pi}{5}\right) & \cos\left(\theta_m - \frac{8\pi}{5}\right) \\ \sin(\theta_m) & \sin\left(\theta_m - \frac{2\pi}{5}\right) & \sin\left(\theta_m - \frac{4\pi}{5}\right) & \sin\left(\theta_m - \frac{6\pi}{5}\right) & \sin\left(\theta_m - \frac{8\pi}{5}\right) \\ \cos(\theta_m) & \cos\left(\theta_m - \frac{6\pi}{5}\right) & \cos\left(\theta_m - \frac{12\pi}{5}\right) & \cos\left(\theta_m - \frac{18\pi}{5}\right) & \cos\left(\theta_m - \frac{24\pi}{5}\right) \\ \sin(\theta_m) & \sin\left(\theta_m - \frac{6\pi}{5}\right) & \sin\left(\theta_m - \frac{12\pi}{5}\right) & \sin\left(\theta_m - \frac{18\pi}{5}\right) & \sin\left(\theta_m - \frac{24\pi}{5}\right) \\ \frac{1}{2} & \frac{1}{2} & \frac{1}{2} & \frac{1}{2} & \frac{1}{2} \end{bmatrix}. \quad (12)$$

Similarly, by multiplying the rotor voltage matrix equation by the transformation matrix $[A_S]$ and adjustment, one obtains the rotor voltage equations in the system $(\alpha\beta xy0)$:

$$\begin{aligned} u_{ar} &= R_R i_{ar} + \frac{d\psi_{ar}}{dt} + \omega_m \psi_{\beta r} \\ u_{\beta sr} &= R_S i_{\beta r} + \frac{d\psi_{\beta r}}{dt} + \omega_m \psi_{ar}. \end{aligned} \quad (13)$$

4 Transformation of linkage magnetic fluxes

To transform the stator matrix equation of the linkage magnetic fluxes in Equation (8) one needs to multiply by the transformation matrix $[A_S]$ from the left as follow:

$$[A_S][\psi_{abcde}] = [A_S][L_S][i_{abcde}] + L_{aA}[A_S][C][i_{ABCDE}]. \quad (14)$$

After the solving, one obtains:

$$\begin{aligned} \psi_{as} &= L_s i_{as} + L_{sr} i_{ar} \\ \psi_{\beta s} &= L_s i_{\beta s} + L_{sr} i_{\beta r} \\ \psi_{xs} &= L_{xs} i_{xs} \\ \psi_{ys} &= L_{ys} i_{ys} \\ \psi_{0s} &= L_{0s} i_{0s}, \end{aligned} \quad (15)$$

where:

$$\begin{aligned} L_s &= L_a - L_{ab} \\ L_{0s} &= L_a + 2L_{ab} \\ L_{xs} &= L_a + 3L_{ab} \\ L_{ys} &= L_a + 3L_{ab} \\ L_{sr} &= \frac{5}{2}L_{aA}. \end{aligned}$$

The transformation of the rotor matrix equation is performed in the same way. One needs to again multiply the rotor matrix equation of the linkage magnetic fluxes in Equation (8) by the transformation matrix $[A_R]$ from the left:

$$[A_R][\psi_{ABCDE}] = L_{aA}[A_R][C][i_{abcde}] + [A_R][L_R][i_{ABCDE}]. \quad (16)$$

After the solving, one obtains:

$$\begin{aligned} \psi_{ar} &= L_R i_{ar} + L_{sr} i_{as} \\ \psi_{\beta r} &= L_R i_{\beta r} + L_{sr} i_{\beta s} \\ \psi_{xr} &= L_{xr} i_{xr} \\ \psi_{yr} &= L_{yr} i_{yr} \\ \psi_{0r} &= L_{0r} i_{0r}, \end{aligned} \quad (17)$$

where:

$$\begin{aligned} L_R &= L_A - L_{AB} \\ L_{0r} &= L_A + 2L_{AB} \\ L_{xr} &= L_A + 3L_{AB} \\ L_{yr} &= L_A + 3L_{AB} \\ L_{sr} &= \frac{5}{2}L_{aA}. \end{aligned}$$

Since in a symmetrical voltage supply system the following is valid: $i_{xs} = i_{ys} = i_{0s} = i_{xr} = i_{yr} = i_{0r} = 0$,

So even: $\psi_{xs} = \psi_{ys} = \psi_{0s} = \psi_{xr} = \psi_{yr} = \psi_{0r} = 0$.

For the linkage magnetic fluxes one can write the following matrix equations:

$$\begin{bmatrix} \psi_{as} \\ \psi_{ar} \end{bmatrix} = \begin{bmatrix} L_s & L_{sr} \\ L_{sr} & L_r \end{bmatrix} \begin{bmatrix} i_{as} \\ i_{ar} \end{bmatrix} \quad (18)$$

$$\begin{bmatrix} \psi_{\beta s} \\ \psi_{\beta r} \end{bmatrix} = \begin{bmatrix} L_s & L_{sr} \\ L_{sr} & L_r \end{bmatrix} \begin{bmatrix} i_{\beta s} \\ i_{\beta r} \end{bmatrix}, \quad (19)$$

5 Electromagnetic torque equation

The equation for the electromagnetic torque of a five-phase motor can be derived from the power in the air gap:

$$M = \frac{5}{2}pL_{sr}(i_{\beta s}i_{ar} - i_{as}i_{\beta r}). \quad (20)$$

To build a dynamic model of the motor, one also needs a mechanical equation:

$$M - M_p = J \frac{d\omega_m}{dt}, \quad (21)$$

where: J is the inertia moment recalculated on the motor shaft, M_p is the load torque.

6 Control of the induction motor (IM)

To control the IM, classical scalar method in an open control loop was used. At the scalar method, the induction motor speed is controlled by setting the voltage and frequency of the stator, so that the magnetic field in the gap is maintained at the desired value. To maintain a constant magnetic field in the gap, U/f ratio must be constant at different motor speeds, [14].

At low speed, it is necessary to compensate the voltage drop across the stator resistance, therefore, the U/f ratio at low speed is set higher than the rated value. For the simulation purposes, the ratio was replaced by a parabolic waveform (Figure 3).

The parabolic waveform can be expressed, using the frequency range (-50,50) Hz and the minimum voltage U_{\min} , according to the relation:

$$u = \frac{46f}{500} + U_{\min} \quad (22)$$

7 Induction motor model in Matlab

To investigate the dynamic properties of the motor, a dynamic model was created in the Matlab-Simulink environment. A block diagram of the drive with a five-phase induction motor is shown in Figure 4. The model was developed based on real measured values on a real

two-pole five-phase motor. The following data were used in the structure of the dynamic model, [11, 15]:

$$\begin{aligned} P_n &= 1.95 \text{ kW}; U_n = 200 \text{ V}/50 \text{ Hz}; p = 1; \\ n_n &= 2910 \text{ rev/min}; R_1 = 3.778 \Omega; R'_2 = 2.498 \Omega; \\ L_m &= 0.436 \text{ H}; L_{1\sigma} = 6.83 \text{ mH}; L'_{2\sigma} = 11.88 \text{ mH}; \\ J &= 0.01 \text{ kgm/s}^2. \end{aligned}$$

The stator linkage magnetic fluxes are calculated based on Equations (11). However before doing that, one needs to transform the five-phase supply voltages into a two-phase system (α, β) in block expressed as 5/2:

$$\begin{aligned} \psi_{\alpha s} &= \int (u_{\alpha s} - R_s i_{\alpha s}) dt \\ \psi_{\beta s} &= \int (u_{\beta s} - R_s i_{\beta s}) dt. \end{aligned} \quad (23)$$

The rotor linkage magnetic fluxes are calculated based on Equations (13) (block Psr), for a motor with a squirrel-cage rotor, $u_{ar} = u_{\beta r} = 0$.

$$\begin{aligned} \psi_{\alpha r} &= \int (-R_r i_{\alpha r} - \omega_m \psi_{\beta r}) dt \\ \psi_{\beta r} &= \int (-R_r i_{\beta r} - \omega_m \psi_{\alpha r}) dt \end{aligned} \quad (24)$$

The stator and rotor currents components are calculated from matrix Equations (19):

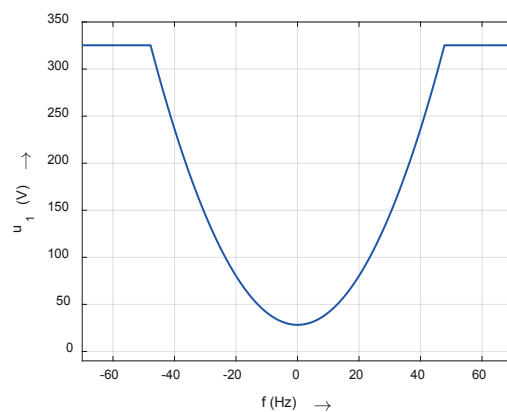


Figure 3 Voltage versus frequency

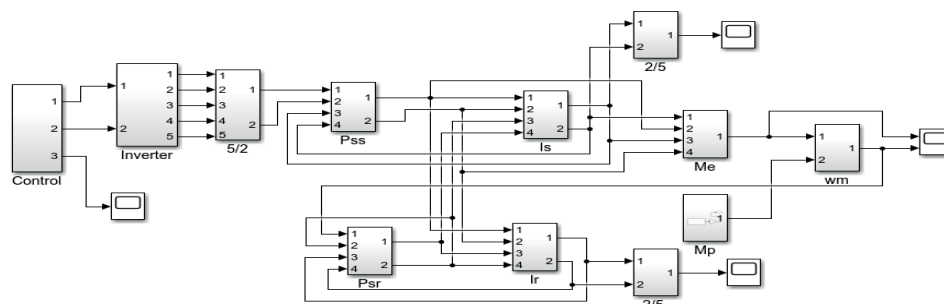


Figure 4 Block diagram of the five-phase IM drive

$$\begin{aligned} i_{as} &= \frac{L_r}{L_s L_r - L_{sf}^2} \psi_{as} - \frac{L_{sf}}{L_s L_r - L_{sf}^2} \psi_{ar} \\ i_s &= \frac{L_r}{L_s L_r - L_{sf}^2} \psi_{\beta s} - \frac{L_{sf}}{L_s L_r - L_{sf}^2} \psi_{\beta r}, \end{aligned} \quad (25)$$

$$\begin{aligned} i_{ar} &= \frac{L_r}{L_s L_r - L_{sf}^2} \psi_{ar} - \frac{L_{sf}}{L_s L_r - L_{sf}^2} \psi_{as} \\ i_r &= \frac{L_r}{L_s L_r - L_{sf}^2} \psi_{\beta r} - \frac{L_{sf}}{L_s L_r - L_{sf}^2} \psi_{\beta s}, \end{aligned} \quad (26)$$

The electromagnetic torque of the motor is calculated based on the Equation (20).

The motor speed is calculated by integrating the Equation (21):

$$\omega_m = \frac{1}{J} \int (M - M_p) dt. \quad (27)$$

8 Simulation results

Using the MATLAB simulation model of a five-phase induction motor, some dynamic states of the drive were simulated. The motor works in an open control loop with control of the voltage-frequency ratio.

Figure 5 shows the waveform of an electromagnetic torque and speed of the motor under frequency start-up and load change. The frequency of the supply voltage during start-up increases linearly from zero to a value of $f = 50$ Hz for $t = 1$ s. The motor is not loaded during a start-up. After the start-up the motor is loaded with a torque equal to the nominal value of the machine ($m_p = 6.5$ Nm). Subsequently, the load torque is reduced to the value of $m_p = 3$ Nm. The corresponding stator and rotor current waveforms are shown in Figure 6. The rotor current value is recalculated to stator.

Figure 7 shows the frequency run-up of a motor

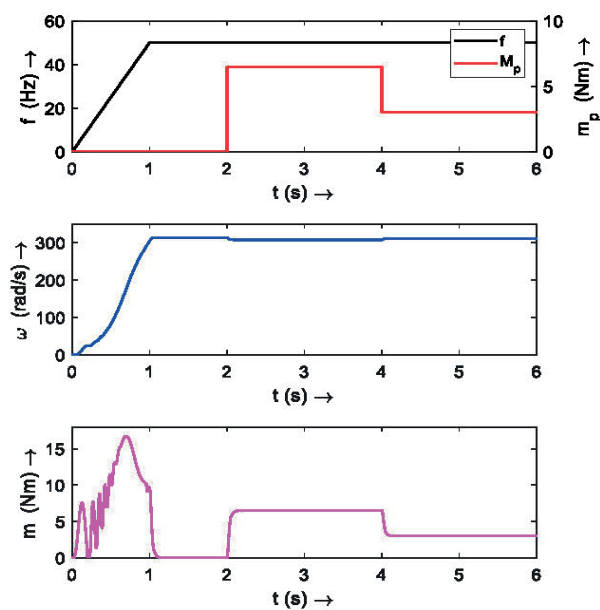


Figure 5 Not loaded motor frequency start-up

loaded with a constant torque of 3 Nm at a frequency of 50 Hz. During the start-up, the ratio U/f is kept constant (Figure 3). Subsequently, the motor is started at a frequency of 80 Hz. In this region, the supply voltage is already independent of frequency and is equal to the nominal value. In Figure 8, the corresponding values of the stator and rotor currents are shown.

Figure 9 shows the simulation results of the frequency reversal drive. The motor is started with a load of 3 Nm at a frequency of 50 Hz. After the start-up, the supply frequency is linearly changed to -50 Hz. During the reversal, the ratio U/f is kept constant. Figure 10 shows the stator and rotor current waveforms during motor reversal, respectively.

9 Conclusion

In the research presented in this paper, a mathematical model of a five-phase induction motor with a squirrel-cage rotor and star-connected stator winding is developed. However, the derived equations are also applicable to pentagonal and pentagram connection systems.

Several typical dynamic states of the motor are demonstrated using the proposed model. The machine's transient behavior is illustrated through the waveforms of stator and rotor phase currents, electromagnetic torque, and speed under various loading conditions.

The motor's characteristics during the frequency ramp-up, reversal, and sudden load application, in the regions of constant torque and constant power operation, are presented.

By comparing the simulation results to waveforms measured on a real five-phase motor drive - previously

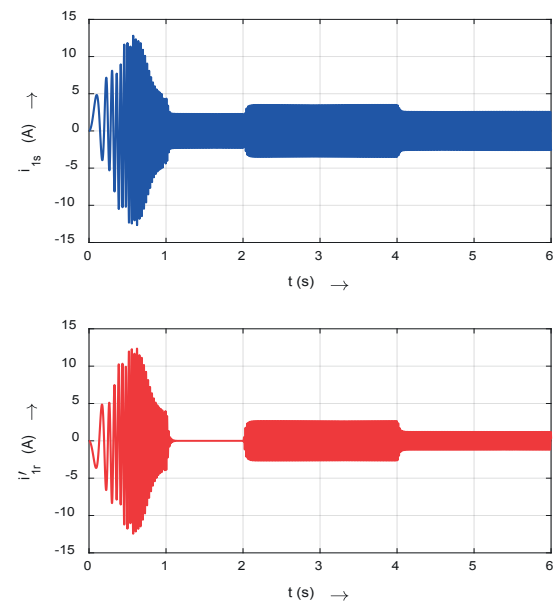


Figure 6 Stator and rotor phase-current

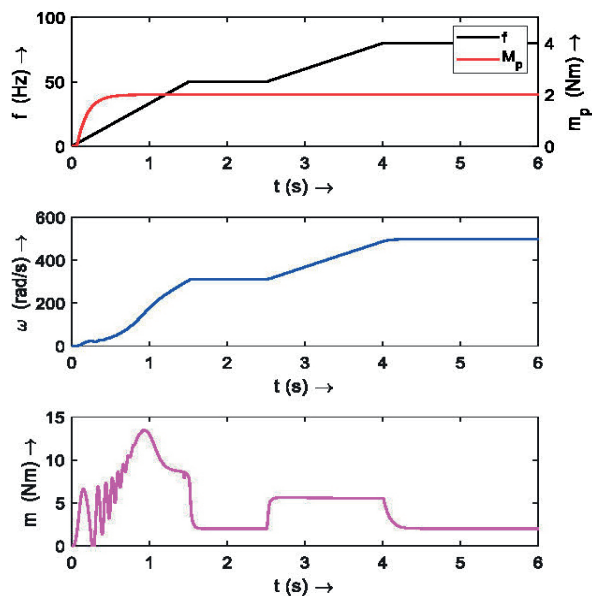


Figure 7 Loaded motor frequency start-up

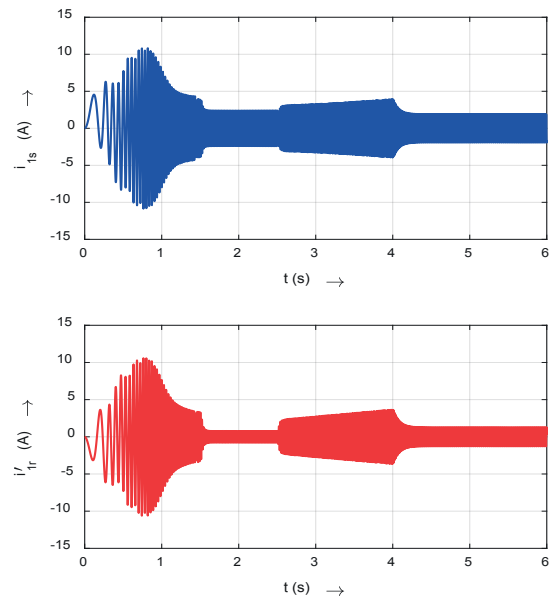


Figure 8 Stator and rotor phase-current

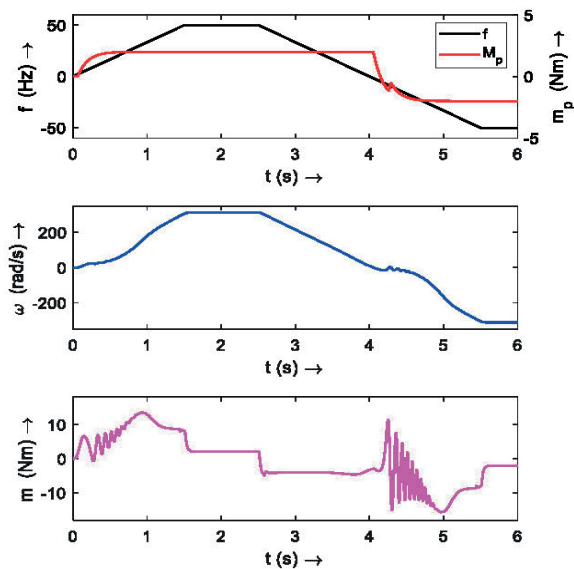


Figure 9 Motor frequency reversal

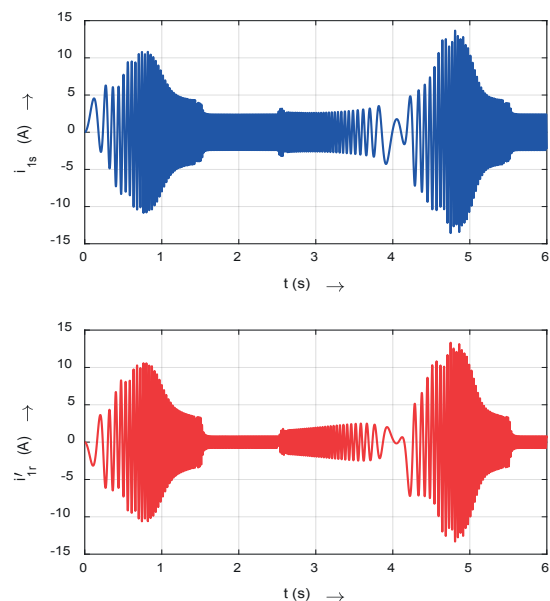


Figure 10 Stator and rotor phase-current

published in [11] - it is concluded that the model is sufficiently accurate and suitable for investigating various dynamic states of the machine. Thus, the proposed model may be accepted as a simulation model, capable of replicating the different operating conditions of an actual motor operating in an industrial environment.

The presented computer simulation model is effective for transient analysis of the five-phase induction motor. Using the SIMULINK software, each block of the model may be connected and modified easily. Some limit conditions, such as saturation of magnetic circuit and stator current limit, may be easily inserted in the function blocks.

Acknowledgment

This work was supported by project APVV-19-0210, project VEGA 1/0363/23 and by the EU Next Generation EU through the Recovery and Resilience Plan for Slovakia under the project No. 09I05-03-V02-00018.

Conflicts of interest

The authors declare that they have no known competing financial interests or personal relationships that could have appeared to influence the work reported in this paper.

References

- [1] SPANIK, P., DOBRUCKY, B., FRIVALDSKY, M., DRGONA, P. Measurement of switching losses in power transistor structure. *Elektronika ir Elektrotechnika / Electronics and Electrical Engineering*. 2008, **2**, p. 75-78. ISSN 1392-1215.
- [2] KELLNER, J., PRAZENICA, M. Research into the possibility of improving the efficiency and torque ripple of a drive with a five-phase induction motor by changing the control in a fault state. In: 2022 International Symposium on Power Electronics, Electrical Drives, Automation and Motion SPEEDAM 2022: proceedings. 2022. p. 663-670.
- [3] KELLNER, J., KASCAK, S., FERKOVA, Z. Investigation of the properties of a five phase induction motor in the introduction of new fault-tolerant control. *Applied Sciences* [online]. 2022, **12**(4), 2249. eISSN 2076-3417. Available from: <https://doi.org/10.3390/app12042249>
- [4] CHOMAT, M., SCHREIER, L. Investigation of induction machine with rotor-bar faults. In: International Conference on Electrical Drives and Power Electronics: proceedings [online]. IEEE. 2019. eISBN 978-1-7281-0389-1, eISSN 1339-3944, p. 12-17. Available from: <https://doi.org/10.1109/EDPE.2019.8883888>
- [5] HOLY, T. Mathematical models of multiphase machines based on symmetrical components decomposition in relation to space harmonics. In: 24-th International Scientific Conference on Electric Power Engineering, EPE 2024: proceedings. 2024.
- [6] CHOMAT, M., SCHREIER, L. Effect of stator winding configuration on operation of converter fed five-phase induction machine. In: Electric Drives and Power Electronics EDPE: proceedings [online]. IEEE. 2015. eISBN 978-1-4673-7376-0, eISSN 1339-3944. Available from: <https://doi.org/10.1109/EDPE.2015.7325343>
- [7] TIAN, B., LU, R., HU, J. Single line/phase open fault-tolerant decoupling control of a five-phase permanent magnet synchronous motor under different stator connections. *Energies* [online]. 2022, **15**(9), 3366. eISSN 1996-1073. Available from: <https://doi.org/10.3390/en15093366>
- [8] FAN, S., MENG, D., AI, M. Comparison and analysis of the performance of five-phase induction motors with different stator winding connections under open-circuit conditions. *Diangong Jishu Xuebao / Transactions of China Electrotechnical Society* [online]. 2022, **37**(7), p. 1679-1688. ISSN 1000-6753. Available from: <https://doi.org/10.19595/j.cnki.1000-6753.tces.201643>
- [9] KUCZMANN, M., HORVATH, K. Design of feedback linearization controllers for induction motor drives by using stator reference frame models. In: 2021 IEEE 19th International Power Electronics and Motion Control Conference PEMC 2021: proceedings. 2021. p. 766-773.
- [10] DOBRUCKY, B., KASCAK, S., PRAZENICA, M., RESUTIK, P. Direct controlled [3x5] matrix converter supplying 5-phase pentacle IM. In: 13th International Conference ELEKTRO 2020: proceedings [online]. 2020. eISBN 978-1-7281-7542-3. Available from: <https://doi.org/10.1109/ELEKTRO49696.2020.9130228>
- [11] KYSLAN, K., LACKO, M., FERKOVA, Z., ZASKALICKY, P. V/f control of five phase induction machine implemented of DSP using Simulink coder. In: 13th, International Conference ELECTRO 2020: proceedings [online]. 2020. eISBN 978-1-7281-7542-3. Available from: <https://doi.org/10.1109/ELEKTRO49696.2020.9130358>
- [12] CHATELAIN, J. *Electrical machines* (in French). Vol. X. University of Lausanne: Romandy Polytechnic Presses, 1983. ISBN 9782604000020.
- [13] SAIKUMAR, V. V., SATHIVANY, B., SURESH, J. Mathematical modeling of five-phase and three-phase induction motor and their result comparison. *IOP Conference Series: Materials Science and Engineering* [online]. 2020, **981**, 042059. ISSN 1757-899X. Available from: <https://doi.org/10.1088/1757-899X/981/4/042059>
- [14] ZHAO, P., LIPO, T. A. Space vector PWM control of dual-phase induction machine using vector space decomposition. *IEEE Transactions on Industry Applications* [online]. 1995, **31**(5), p. 1100-1109. ISSN 0093-9994, eISSN 1939-9367. Available from: <https://doi.org/10.1109/28.464525>
- [15] ZASKALICKY, P., KANUCH, J. Dynamic model of five-phase induction motor. In: 2023 International Conference on Electrical Drives and Power Electronics EDPE 2023: proceedings [online]. IEEE. 2023. eISBN 979-8-3503-2275-0, eISSN 2770-7652. Available from: <https://doi.org/10.1109/EDPE58625.2023.10274057>